

Microstructure and Phase Chemistry of Vacuum Induction Melting Fabricated-Equimolar AlCoCrFeNi HEA During Spinodal Dissolution Annealing

Mudassar Hussain¹, Abdillah Sani Mohd Najib^{1,2}, Nor Akmal Fadil^{1,2}, Tuty Asma Abu Bakar^{1,2*}

¹ Department of Materials, Manufacturing & Industrial Engineering, Faculty of Mechanical Engineering, Universiti Teknologi Malaysia 81310 UTM Johor Bahru, Johor, MALAYSIA

² Materials Research Consultancy Group (MRCG), Faculty of Mechanical Engineering, Universiti Teknologi Malaysia, 81310 UTM Johor Bahru, Johor, MALAYSIA

*Corresponding Author: tuty@utm.my

DOI: <https://doi.org/10.30880/ijie.2024.16.06.014>

Article Info

Received: 26 August 2024

Accepted: 14 October 2024

Available online: 4 November 2024

Keywords

Equimolar AlCoCrFeNi high entropy alloy (HEA), Al-Ni rich region, dissolution annealing, binodal decomposition, Cr-Fe rich interdendritic region

Abstract

The quinary equimolar AlCoCrFeNi high entropy alloy (HEA) as a promising candidate for advanced engineering applications has grasped significant consideration in recent years due to its ability to undergo tailorable microstructure transformation and properties. The transient understanding of elemental distribution and response to the cooling rate during dissolution annealing and binodal decomposition are still required to evaluate. The present study investigates variations in phase chemistry and microstructure during dissolution annealing at 1h and 16h at 800°C (air cooled) by FESEM-EDS mapping and XRD analysis. Secondly, to identify binodal decomposition in samples annealed at 1250°C for 20h is revealed at different cooling rates (water quenching and furnace cooling) employing FESEM-EDS. Remarkable binodal decomposition was witnessed with distinct phase composition and phase boundaries during slow cooling, while thin interfacial face centered cubic (FCC) phase separation occurred in a rapidly cooled sample. However, heating at 800°C for 1h and 16h revealed modulated microstructure with rearrangements in the chemical composition of phases compared to cast microstructure. Al-Ni rich dendritic region and Cr-Fe rich interdendritic region interdiffusion during dissolution annealing at 800°C with Ni and Cr cross mobilisation. However, Co remains in uniform distribution in both regions. It confirms microstructure tailorability and variance in engineering applicability of quinary equimolar AlCoCrFeNi high entropy alloy with different thermal treatments.

1. Introduction

The era of conventional alloy systems containing one principal element is shaded with a new concept of multi-principal elemental alloys named high entropy alloys (HEA) from the last one and half decades [1]. HEAs are multi-principal element alloys containing at least five elements with a target atomic composition of 5% ~ 35% each [2, 3]. Synergistic properties of high strength, ductility, temperature stability, fracture toughness and corrosion resistance outclass AlCoCrFeNi high entropy alloy system for robust engineering applications [4]. Mohanty et al. have explored the phase development in AlCoCrFeNi high entropy alloys produced by mechanical alloying and subsequent sintering. They have reported the emergence of a tetragonal sigma (σ) phase containing Cr-Fe-Co

while Al-Ni rich L12 ordered α phase and Al-Ni-Co-Fe FCC solid solution phase as a matrix for sample sintered from 699.85 to 999.85°C [5]. As reported by Ji et al., the AlCoCrFeNi high entropy alloy had a two-phase microstructure with BCC and FCC phases. It was produced by mechanical alloying and consolidation under spark plasma sintering at 900°C [6]. However, in cast AlCoCrFeNi HEA, a dendritic solidification pattern is observed with Al-Ni rich phase embedded in a Cr-Fe rich matrix, contrary to that in interdendritic region. While reviewing heat treatment temperature and time impact on phase transformation of equimolar AlCoCrFeNi HEA after initial consolidation via conventional casting or powder metallurgy route, previous study has shown that the sigma (σ) phase (Cr-Fe rich) is frequently generated in the interdendritic (ID) region (Cr-Fe rich) governed by diffusional transformation of BCC to FCC governed by solute rejection of Fe and Cr. For instance, Strumza et al. discovered that the σ phase would transmute into BCC/B2 particles at 960.1°C [7]. The quench sensitivity of any alloy determines its applicability and range of achievable mechanical properties. Like conventional alloys (steels, titanium alloys and aluminium alloys), prospects of equimolar AlCoCrFeNi HEA are required to determine.

Substantial work has been reported on heat treatment of AlCoCrFeNi HEA in different temperature ranges. However, we have focused on determining the alteration in microstructure and its associated variation in phase chemistry in vacuum induction melted equimolar AlCoCrFeNi HEA at transformation temperature of 800°C for 1h and 16h and the influence of cooling rate from high-temperature single phase annealing on phases separation and elemental redistribution.

2. Methodology

2.1 Melting and Casting

An equimolar high entropy alloy AlCoCrFeNi was prepared by using 99.99% pure elements of Al, Co, Cr, Fe and Ni in a vacuum induction melting furnace (VIM). A high vacuum of 10⁻⁵ mbar was maintained initially during melting and casting. Then, high-purity argon gas was purged in the chamber to maintain an atmospheric pressure of 500 ~ 800 mbar to reduce elemental losses. The melt was poured into ceramic mold to solidify. The cast ingot was remelted thrice with 180° axial rotation to maintain compositional homogeneity in the final ingot used for further experimentation. The cast ingot of diameter 50 mm and length 350 mm was cut into cubical pieces 8~10 mm on each side for heat treatment, compositional, and microstructure analysis.

2.2 Composition Analysis, Heat Treatment and Characterization

The quantitative elemental composition of cast ingot was determined by employing PerkinElmer Avio 200 ICP-OES after digestion and dilution process. A comprehensive heat treatment plan was devised based on previous findings by various researchers to determine the σ -phase kinematics over the span of time at the phase transformation temperature, as shown in Fig. 1 [8, 9]. Cubical samples were cold mounted, ground and polished to examine under field emission scanning electron microscope (FESEM) HITACHI SU8020 for microstructure analysis and elemental mapping by BRUKER X-ray detector using electron deceleration mod for imaging due to ferromagnetic nature of material and low acceleration voltage of 0.5kV while for EDS mapping acceleration voltage was increased to 20kV. for determining the phase constituents and their evolution over the temperature range and exposure time in cast and heat treated equimolar AlCoCrFeNi HEA. The XRD was conducted using Rigaku Smart Lab (45KV-200mA) with Cu- α radiation ($\lambda=1.5406\text{nm}$) at a scanning rate of 1/min, step size of 0.02°, and within 2 θ angle range of 20 to 100°. The diffraction patterns measured were used for the investigations of crystal structure.

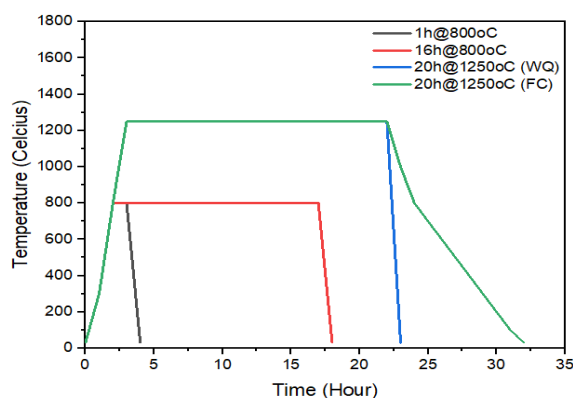


Fig. 1 Heat treatment cycle of equimolar AlCoCrFeNi HEA

3. Results and Discussion

3.1 Chemical Composition

ICP-OES compositional analysis was conducted to verify the equimolar composition of AlCoCrFeNi high entropy alloy. Its results suggest a composition drift from ideal equimolar composition because iron (Fe) contents are reported as the highest while aluminium (Al) is on the lowest side of compositional range. However, it still validates its nearly equimolar composition, as mentioned in Table 1.

Table 1 Chemical composition of Equimolar AlCoCrFeNi HEA

Sr. No.	Element	Composition at %
1	Al	17.46+0.018
2	Co	19.61+0.019
3	Cr	19.86+0.020
4	Fe	21.97+0.022
5	Ni	21.09+0.021

3.2 Microstructure Analysis and Phase Chemistry

As-cast AlCoCrFeNi HEA: The microstructure of the cast is distinctly divided into two components: the interconnected dendritic structure arranged in a weaving pattern and the interdendritic area characterised by the presence of cuboidal particles dispersed throughout. Fig. 2. illustrates the elemental distribution inside the dendritic zone, including a region rich in Al-Ni, whereas Co is expected to exhibit uniform dispersion. In the interdendritic zone, the concentrations of chromium (Cr) and iron (Fe) exhibit comparatively greater levels than those in the dendritic region, but cobalt (Co) remains mostly unaltered. According to the research conducted by Einat Strumza and colleagues, the Al-Ni-rich area in its as-cast state has a body-centred cubic (BCC) crystal structure. Additionally, inside this region, there are interdendritic spinodal-decomposed BCC nano-sized cuboidal particles that are embedded in the ordered B2 phase. These particles demonstrate a preferential co-clustering of Al-Ni and Cr-Fe, as seen in Fig. 3.

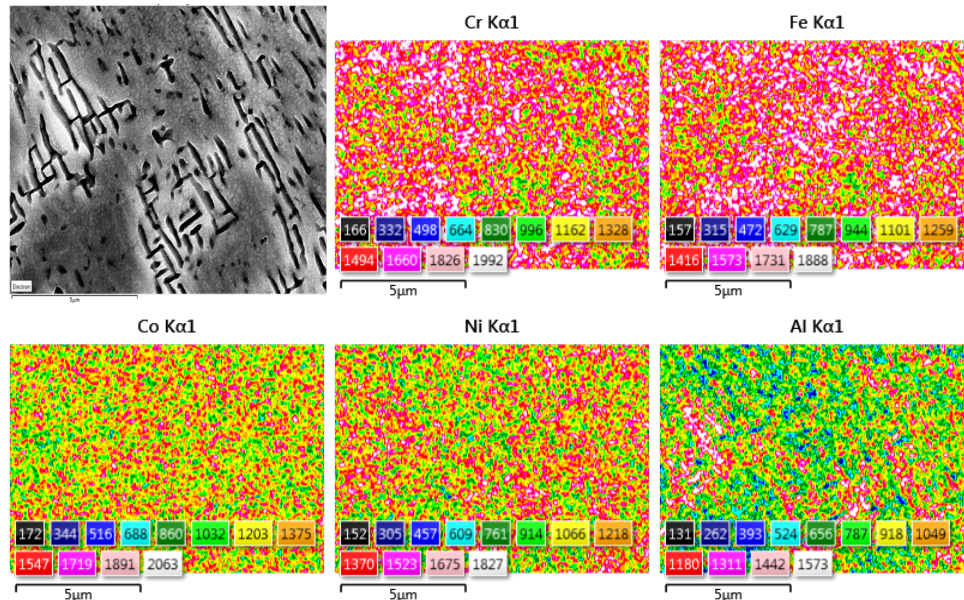


Fig. 2 EDS-mapping of as-cast equimolar AlCoCrFeNi HEA

Spinodal dissolution annealing at 800°C for 1h: Following a heat treatment process at a temperature of 800°C for a duration of 1h, interregional elemental diffusion was seen in the equimolar AlCoCrFeNi high-entropy alloy (HEA). This diffusion process facilitated the co-segregation of chromium (Cr), iron (Fe), and cobalt (Co), as shown by the similarity in X-ray counts per second observed in the intensity pattern of the elemental mapping given in Fig. 4. In contrast, Al tends to form clusters, but Ni demonstrates a uniform diffusion across the microstructure, contrary to its starting state.

Spinodal dissolution annealing at 800°C for 16h: The cast AlCrCrFeNi high-entropy alloy (HEA) was subjected to a heat treatment at a temperature of 800°C for 16h, as shown in Fig. 5. This treatment resulted in the preservation of the analogous elemental distribution pattern, hence proving the presence of co-segregation areas

consisting of Al-Ni and Cr-Fe-Co in both dendritic and interdendritic regions. At the boundary between dendritic and interdendritic regions, the concentrations of chromium (Cr) and iron (Fe) are seen to be elevated in comparison to the other areas of the energy-dispersive spectroscopy (EDS) mapping. This observation aligns with the previous research conducted by Louisa Meshi et al., which specifically pertains to the region where the sigma (σ) phase is known to occur [10]. The AlCrCrFeNi high-entropy alloy (HEA) specimen was exposed to a thermal condition of 800°C for 16h, as seen in Fig. 5. The experiment yielded consistent results, demonstrating the presence of co-segregation zones of Al-Ni and Cr-Fe-Co in both dendritic and interdendritic areas. At the interface between dendritic and interdendritic regions, the concentrations of chromium (Cr) and iron (Fe) exhibit greater values compared to the other sections of the energy-dispersive spectroscopy (EDS) mapping. This discovery is consistent with the findings reported by Louisa Meshi et al., who identified this region as where the sigma (σ) phase is found [10].

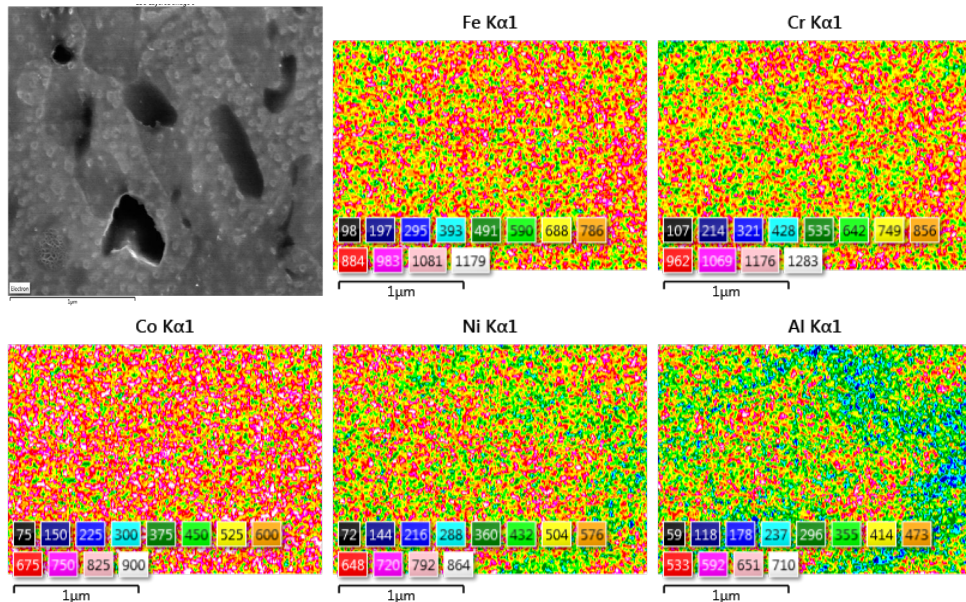


Fig. 3 EDS-mapping of as-cast interdendritic region of equimolar AlCoCrFeNi HEA

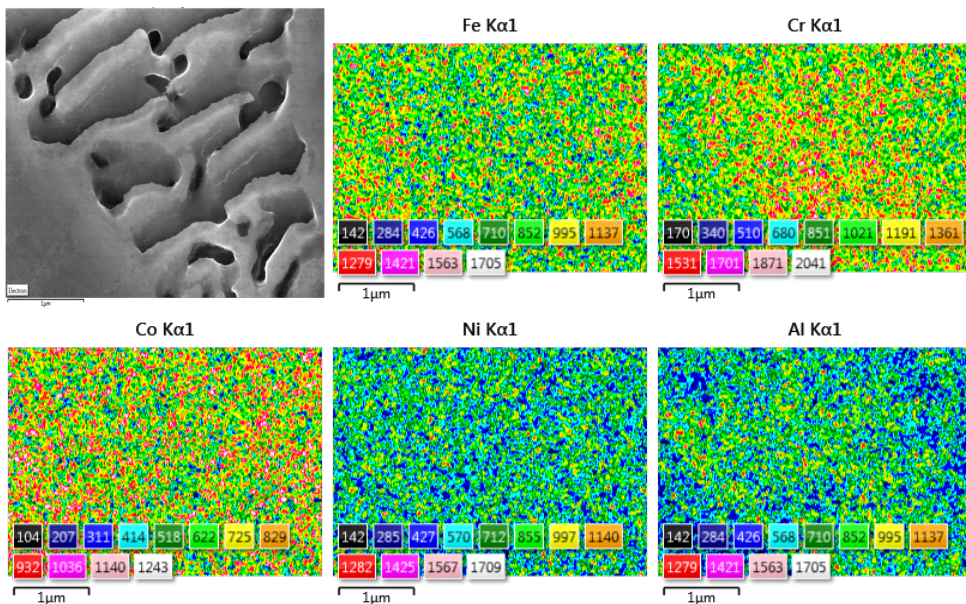


Fig. 4 EDS-mapping of equimolar AlCoCrFeNi HEA heat-treated at 800°C for 1h

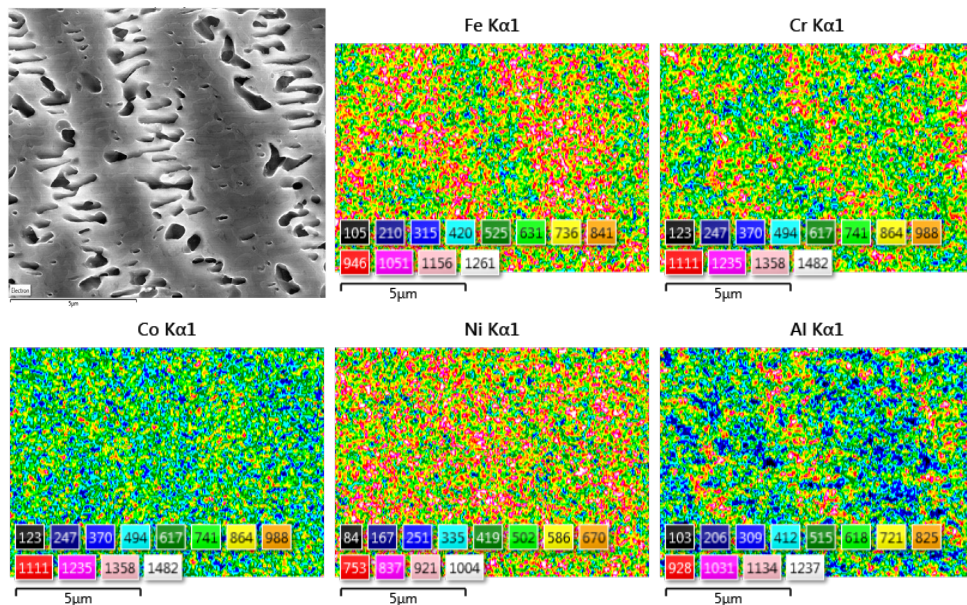


Fig. 5 EDS-mapping of equimolar AlCoCrFeNi HEA heat-treated at 800°C for 16h

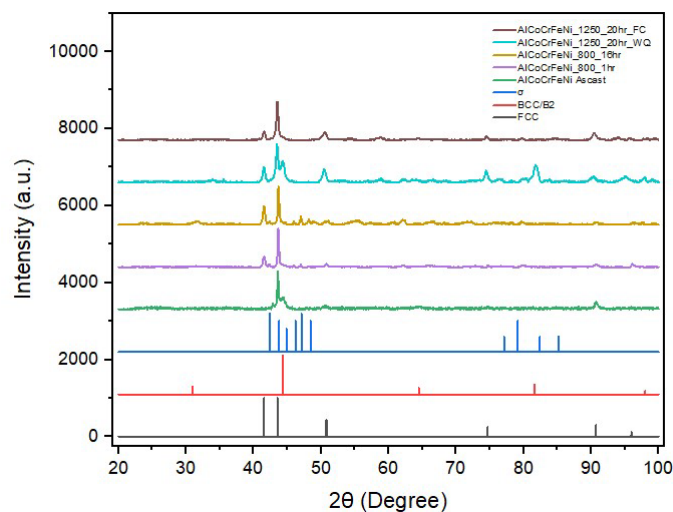


Fig. 6 XRD pattern of AlCoCrFeNi HEA in different condition

Spinodal dissolution annealing at 1250°C for 20h and water quenched: The process of homogenisation in a single phase has been extensively studied by Zhao et al. In their research, they observed the disappearance of sigma (σ) and FCC phases in an equimolar AlCoCrFeNi high-entropy alloy (HEA) [11]. Therefore, the experiment was carried out at 1250°C for 20h. One of the specimens that was rapidly cooled in water has a proclivity for an inherently unstable body-centred cubic (BCC) phase, displaying the characteristic eutectoid phase change at the boundary between dendritic and interdendritic regions (Fig. 7). Upon rapid cooling in water at the homogenisation temperature, a thin interfacial face-centred cubic (FCC) phase, characterised by an increased concentration of aluminium (Al) and nickel (Ni), was observed, as seen in Fig. 6&7. [12]. The interdendritic zone has a greater concentration of chromium (Cr) and iron (Fe), while the dendritic region shows elevated levels of aluminium (Al) and nickel (Ni) in comparison to its counterpart.

Spinodal dissolution annealing at 1250°C for 20h and furnace cooled: Nevertheless, the experimental results obtained from a sample cooled in a furnace and analysed by EDS mapping in a field emission electron microscope (FESEM) provided evidence for the influence of cooling rate on phase separation. A pronounced sinusoidal pattern of element distribution has been observed [13]. The presence of sigma (σ) phase recurrence may be shown in the interdendritic area using EDS mapping, where a significant increase in Cr and Fe contents is evident in Fig. 7. However, this observation was not corroborated by the XRD analysis, as shown in Fig. 6. Upon doing a more detailed examination of the dendritic region to map the elemental composition (as seen in Fig. 9), it becomes evident that there are two clearly defined areas consisting of Al-Ni and Cr-Fe-rich phases. These phases exhibit a complex arrangement characterised by a rectilinear tangled pattern. Furthermore, the interdendritic region,

which is rich in Cr-Fe, displays additional co-clustering of Cr-Fe-Co and Al-Ni phases. According to reference [14], the interdendritic area rich in chromium, iron, and cobalt, and with the lowest aluminium content, is susceptible to the formation of the sigma (σ) phase when subjected to gradual cooling from the homogenisation temperature, as seen in Fig. 10.

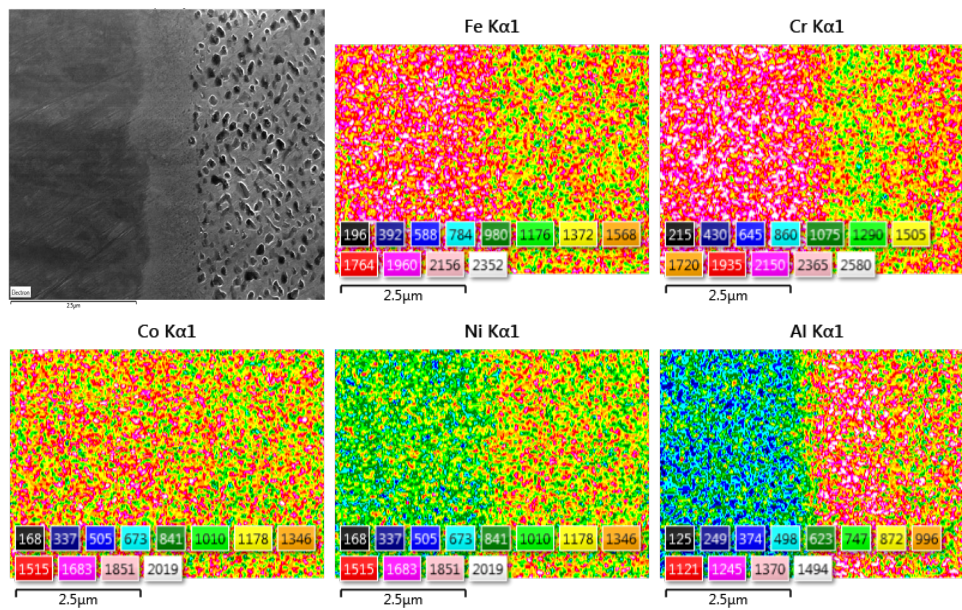


Fig. 7 EDS-mapping of equimolar AlCoCrFeNi HEA heat-treated at 1250°C for 20h and water quenched

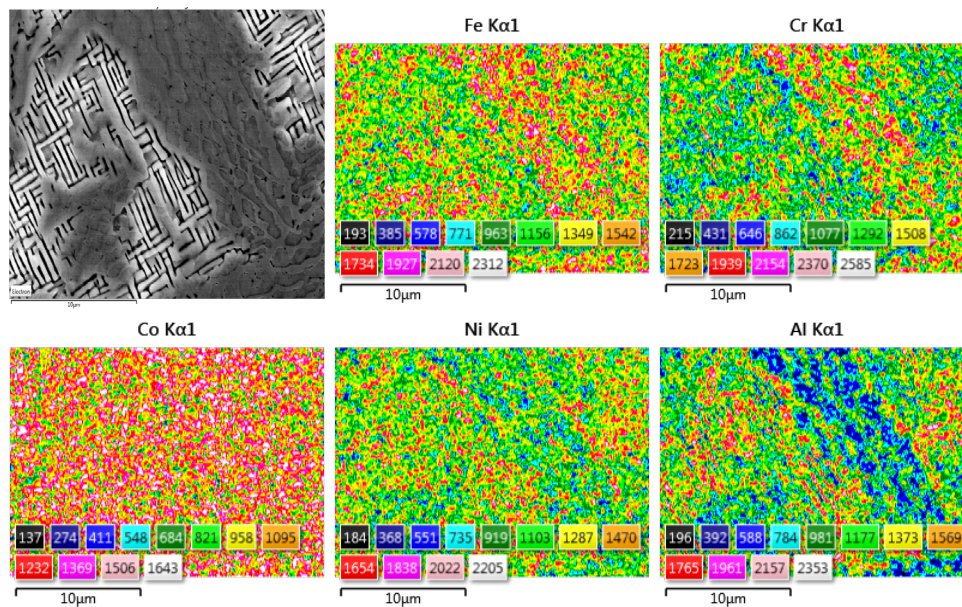


Fig. 8 EDS-mapping of equimolar AlCoCrFeNi HEA heat-treated at 1250°C for 20h and furnace-cooled

The Equimolar AlCoCrFeNi high-entropy alloy has garnered significant attention in the field of high-entropy alloys (HEAs) due to its microstructure and phase transition characteristics, which bear resemblance to those seen in steels and titanium alloys. Contrary to traditional alloy systems, these materials demonstrate exceptional mechanical capabilities, great temperature stability and resistance to corrosion. The microstructure in the as-cast state has a dendritic morphology, with a zone between the dendrites rich in chromium and iron and a dendritic area rich in aluminium and nickel. This observation is consistent with findings reported in prior investigations. The X-ray diffraction (XRD) investigation reveals the presence of faint peaks that correspond to the L12 Al-Ni phase, in addition to the B2 phase. This observation contradicts the findings reported by Zhang et al. [15]. High-entropy alloys are characterised by a notable deceleration in diffusion rates compared to their dilute conventional alloy counterparts. This phenomenon may be attributed to changes in the alloying elements' atomic size and atomic percentage. The limited atomic mobility of chromium (166 pm) and iron (156 pm) is facilitated by their somewhat larger atomic radii compared to aluminium (118 pm) and nickel (149 pm), resulting in a slow diffusion

process. The interdendritic area located at the border between interfaces experiences an enrichment in chromium (Cr) and iron (Fe) concentrations when the lattice parameters rise at elevated temperatures.

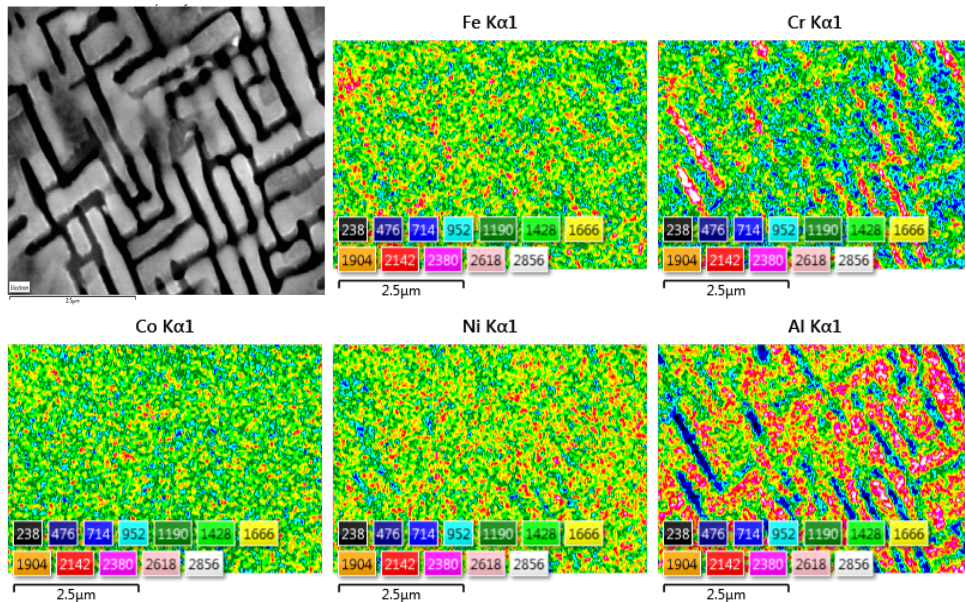


Fig. 9 EDS-mapping of the dendritic region of heat-treated sample at 1250°C for 20h and furnace-cooled

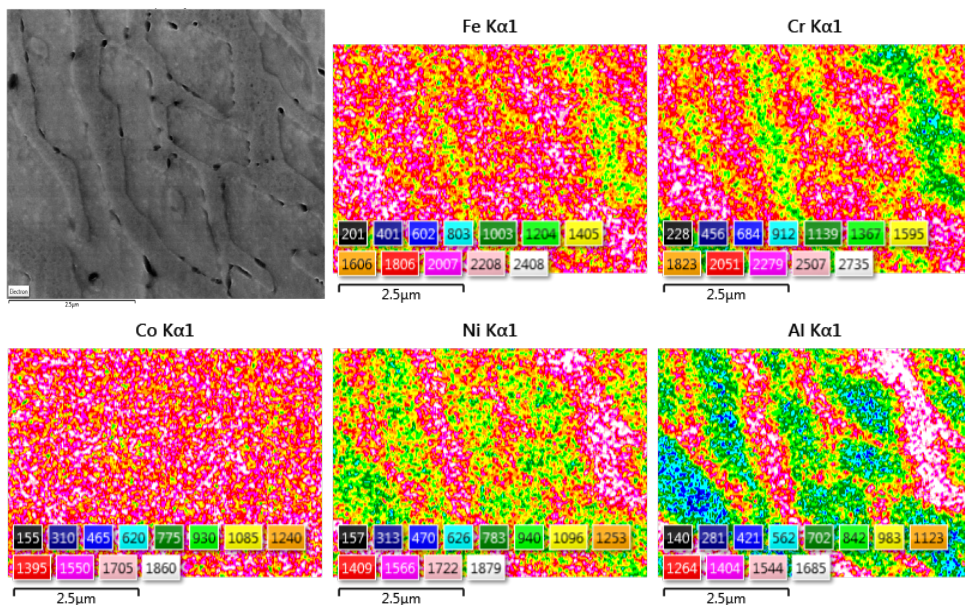


Fig. 10 EDS-mapping of the interdendritic region of heat-treated sample at 1250°C for 20h and furnace-cooled

There is a notable similarity between the phases seen in the water-quenched sample from a temperature of 1250°C, as described in this study, and the findings published by Zhao et al. and Muntiz et al. [16, 17]. However, it is important to note that our results contradict the claims made by Zhang et al. and Wang et al. [12, 18]. The presence of the intergranular face-centred cubic (FCC) phase in the equimolar AlCoCrFeNi high-entropy alloy (HEA) serves as evidence for the alloy's susceptibility to quenching, as opposed to maintaining the body-centred cubic (B2/BCC) phase. The presence of localised nanosized co-segregation of Cr-Fe-rich clusters within the precipitation FCC phase has raised interest in understanding the mechanism behind the development of the FCC phase upon cooling from a temperature of 1250°C. During the process of cooling the sample in a furnace environment at a temperature of 1250°C, a significant occurrence of precipitation of the Al-Ni-rich interdendritic face-centred cubic (FCC) phase was observed. The observable spinodal breakdown takes place at the homogenisation temperature, forming a rectilinear woven network consisting of interlaminated regions of Cr-Fe and Al-Ni-rich phases inside the dendritic area [11, 17, 19, 20]. Nevertheless, the area between dendrites, known as the interdendritic region, has a higher concentration of Cr-Fe compared to the dendritic zone. This region displays a morphology like a river-land formation, with Al-Ni-rich face-centred cubic (FCC) and Cr-Fe-rich B2

phases. The elemental distribution seen in the high-temperature B2/BCC phase does not promote the formation of the tetragonal sigma (σ) phase, in contrast to the as-cast B2/BCC phase. The observed irreversibility of the tetragonal sigma (σ) phase upon cooling from high temperatures contradicts the current understanding of this phase in stainless steels and Fe-Cr-rich conventional alloys.

4. Conclusion

The as-cast sample exhibits two distinct regions: dendritic Al-Ni rich and interdendritic Cr-Fe rich. However, Co is homogeneously distributed in both regions. Both regions can be further divided into Al-Ni rich and Cr-Fe rich phases. While exposing at 800°C for 1h and 16h, the morphology of dendritic and interdendritic regions alters, and Ni from dendritic region diffuses to interdendritic zone while Cr diffuses from interdendritic region to dendritic zone. However, Al, Fe and Co hold their as-cast concentration profile. On water quenching followed by annealing 1250°C for 20h signifies the immiscibility gap among the phases and appears into dendritic, interdendritic and interfacial diffusion zones enriched with Cr-Fe, Al-Ni and Cr-Fe, respectively. This interfacial zone disappears during furnace cooling from 1250°C, representing unstable transient stage of binodal decomposition. Phase separation in sample heat treated at 1250°C and furnace cooled is more pronounced than in a solidified structure, making the structure more stable. Improvement in chemical homogeneity of equimolar AlCoCrFeNi HEA during dissolution annealing at 800°C, formation of metastable structure during water quenching from 1250°C, and remarkable phase separation during furnace cooling from 1250°C signifies the tailor ability of microstructure and associated properties of alloy.

Acknowledgement

This work is funded by the Ministry of Higher Education under the Fundamental Research Grant Scheme (FRGS), Registration Proposal No: FRGS/1/2022/TK10/UTM/02/45.

Conflict of Interest

Authors declare that there is no conflict of interests regarding the publication of the paper.

Author Contribution

The authors confirm contribution to the paper as follows: **Conceptualization, material fabrication, experimentation, acquisition of results, their analysis and drafting of paper:** Mudassar Hussain; **Reviewed, critically analysed, supervised and discussed results:** Abdillah Sani Mohd Najib, Nor Akmal Fadil and Tuty Asma Abu Bakar.

References

- [1] Chen, H.Y., et al., (2006) Effect of the substitution of Co by Mn in Al-Cr-Cu-Fe-Co-Ni high-entropy alloys. *Annales De Chimie-Science Des Materiaux*, **31**(6): p. 685-698. <https://doi.org/10.3166/acsm.31.685-698>
- [2] Cantor, B., et al., (2004) Microstructural development in equiatomic multicomponent alloys. *Materials Science and Engineering: A*, **375-377**: p. 213-218. <https://doi.org/10.1016/j.msea.2003.10.257>
- [3] Yeh, J.W., et al., (2004) Nanostructured high-entropy alloys with multiple principal elements: novel alloy design concepts and outcomes. *Advanced engineering materials*, **6**(5): p. 299-303. <https://doi.org/10.1002/adem.2003300567>
- [4] Yeh, J.-W., (2013) Alloy Design Strategies and Future Trends in High-Entropy Alloys. *Jom*, **65**(12): p. 1759-1771 <https://doi.org/10.1007/s11837-013-0761-6>
- [5] Mohanty, S., et al., (2017) Powder metallurgical processing of equiatomic AlCoCrFeNi high entropy alloy: Microstructure and mechanical properties. *Materials Science and Engineering: A*, **679**: p. 299-313 <https://doi.org/10.1016/j.msea.2016.09.062>
- [6] Ji, W., et al., (2014) Mechanical alloying synthesis and spark plasma sintering consolidation of CoCrFeNiAl high-entropy alloy. *Journal of Alloys and Compounds*, **589**: p. 61-66. <https://doi.org/10.1016/j.jallcom.2013.11.146>
- [7] Strumza, E., et al., (2022) A comprehensive study of phase transitions in Al_{0.5}CoCrFeNi high-entropy alloy at intermediate temperatures (400≤T≤900° C). *Journal of Alloys and Compounds*, **898**: p. 162955 <https://doi.org/10.1016/j.jallcom.2021.162955>
- [8] Zhou, Y.-k., et al., (2022) Effect of vacuum heat treatment on microstructure and mechanical properties of HVOF sprayed AlCoCrFeNiCu high-entropy alloy coating. *Materials Letters*, **323**. <https://doi.org/10.1016/j.matlet.2022.132551>

- [9] Zhang, X., et al., (2022) The phase composition characteristics of AlCoCrFeNi high entropy alloy heat-treated by simple normalizing treatment and its effects on mechanical properties. *Journal of Alloys and Compounds*, **926**: p. 166-196. <https://doi.org/10.1016/j.jallcom.2022.166896>
- [10] Meshi, L., et al., (2019) Retardation of the σ phase formation in the AlCoCrFeNi multi-component alloy. *Materials Characterization*, **148**: p. 171-177. <https://doi.org/10.1016/j.matchar.2018.12.010>
- [11] Zhao, C., et al., (2020) Effect of strong magnetic field on the microstructure and mechanical-magnetic properties of AlCoCrFeNi high-entropy alloy. *Journal of Alloys and Compounds*, **820** . <https://doi.org/10.1016/j.jallcom.2019.153407>
- [12] Zhang, X., et al., (2022) The phase composition characteristics of AlCoCrFeNi high entropy alloy heat-treated by simple normalizing treatment and its effects on mechanical properties. *Journal of Alloys and Compounds*, **926**. <https://doi.org/ARTN 16689610.1016/j.jallcom.2022.166896>
- [13] Yen, S.Y., et al., (2022) B2-strengthened Al-Co-Cr-Fe-Ni high entropy alloy with high ductility. *Materials Letters*, **325**. <https://doi.org/10.1016/j.matlet.2022.132828>
- [14] Joseph, J., et al., (2022) Optimising the Al and Ti compositional window for the design of gamma' (L1(2))-strengthened Al-Co-Cr-Fe-Ni-Ti high entropy alloys. *Materials Science And Engineering A-structural materials properties microstructure and processing*, **835**. <https://doi.org/10.1016/j.msea.2022.142620>
- [15] Zhang, X., et al., (2022) The phase composition characteristics of AlCoCrFeNi high entropy alloy heat-treated by simple normalizing treatment and its effects on mechanical properties. *Journal of Alloys and Compounds*, **926**. <https://doi.org/10.1016/j.jallcom.2022.166896>
- [16] Zhao, C., et al., (2020) Tailoring mechanical and magnetic properties of AlCoCrFeNi high-entropy alloy via phase transformation. *Journal of Materials Science & Technology*, **73**: p. 83-90. <https://doi.org/10.1016/j.jmst.2020.08.063>
- [17] Munitz, A., et al., (2016) Heat treatment impacts the micro-structure and mechanical properties of AlCoCrFeNi high entropy alloy. *Journal of Alloys and Compounds*, **683**: p. 221-230. <https://doi.org/10.1016/j.jallcom.2016.05.034>
- [18] Wang, A., et al., (2021) Ultrafast formation of single phase B2 AlCoCrFeNi high entropy alloy films by reactive Ni/Al multilayers as heat source. *Materials & Design*, **206**: p. 109790. <https://doi.org/10.1016/j.matdes.2021.109790>
- [19] Wang, C.T., et al., (2021) Strain Rate Effects on the Mechanical Properties of an AlCoCrFeNi High-Entropy Alloy. *Metals and Materials International*, **27**(7): p. 2310-2318. <https://doi.org/10.1007/s12540-020-00920-5>
- [20] Zhao, C., et al., (2021) Optimizing mechanical and magnetic properties of AlCoCrFeNi high-entropy alloy via FCC to BCC phase transformation. *Journal of Materials Science & Technology*, **86**: p. 117-126 <https://doi.org/10.1016/j.jmst.2020.12.080>